HHS Public Access

Corin is a key regulator of endochondral ossification and bone development via modulation of vascular endothelial growth factor A expression

Rachel C. Nordberg[1], **Hao Wang**[2], **Qingyu Wu**[2], and **Elizabeth G. Loboa**[1,3]

[1]Joint Department of Biomedical Engineering at University of North Carolina at Chapel Hill and North Carolina State University, Raleigh, North Carolina

[2]Molecular Cardiology, Cleveland Clinic, Ohio

[3]College of Engineering, University of Missouri, Columbia, Missouri

Abstract

Corin has been studied extensively within the vascular system and is known to regulate blood pressure. We have shown that corin is one of the most highly upregulated genes during osteogenic differentiation of human adipose-derived stem cells (hASCs). This study tested the hypothesis that, through modulation of angiogenic signalling pathways, corin is a critical regulator of osteogenic differentiation and endochondral ossification. In vitro, corin expression in hASC was suppressed via siRNA knockdown and vascular endothelial growth factor A (VEGF-A) expression was quantified via reverse transcription polymerase chain reaction. In vivo, a murine corin knockout model (female, 10 weeks) was used to determine the effect of corin deficiency on long bone development. Wild-type and corin knockout long bones were compared via haematoxylin and eosin staining to assess tissue characteristics and cellular organization, three-point bending to assess mechanical characteristics, and immunohistochemistry to visualize VEGF-A expression patterns. Corin knockdown significantly ($p < 0.05$) increased VEGF-A mRNA expression during osteogenic differentiation. In vivo, corin knockout reduced tibial growth plate thickness ($p < 0.01$) and severely diminished the hypertrophic region. Corin knockout femurs had significantly increased stiffness ($p < 0.01$) and maximum loads ($p < 0.01$) but reduced postyield deflections ($p < 0.01$). In corin knockout mice, VEGF-A expression was increased near the growth plate but was reduced throughout the tibial shaft and distal head of the tibiae. This is the first study to show that corin is a key regulator of bone development by modulation of VEGF-A expression. Further elucidation of this mechanism will aid in the development of optimized bone tissue engineering and regenerative medicine therapies.

Correspondence: Elizabeth G. Loboa, College of Engineering, University of Missouri, Columbia, MO 65211. egloboa@missouri.edu.

CONFLICT OF INTEREST

The authors have nothing to disclose.

1 | INTRODUCTION

Bone is formed via two main processes in vivo: intramembranous ossification and endochondral ossification. During intramembranous ossification, bone is formed via mesenchymal precursor cells differentiating directly into osteoblasts, which generate bone matrix (Yang et al., 2012). Alternatively, bone can be formed via endochondral ossification. During endochondral ossification, mesenchymal precursor cells differentiate into chondrocytes, which proliferate, generate cartilage matrix, and undergo hypertrophy. Blood vessels and bone cells subsequently invade the cartilage to ossify the tissue and form bone (Mackie, Ahmed, Tatarczuch, Chen, & Mirams, 2008; Yang et al., 2012). Due to the complex nature of skeletal formation and endochondral ossification, many of the signalling mechanisms that direct these processes have yet to be fully elucidated.

Human adipose-derived stem cells (hASCs) have great potential for use in bone tissue engineering applications due to their osteogenic differentiation potential, autologous availability, and immunocompatibility (Gimble, Katz, & Bunnell, 2007; Gomillion & Burg, 2006; Lee et al., 2004; Mizuno, 2009; Nordberg & Loboa, 2015; Schaffler & Buchler, 2007). We previously performed microarray analyses of hASC during osteogenic differentiation in order to determine which genes were the most highly upregulated during osteogenic differentiation. Interestingly, we identified corin, an atrial natriuretic peptide (ANP)-converting enzyme, as one of the most highly upregulated genes during hASC osteogenic differentiation (Charoenpanich et al., 2011). Corin has also been found to be upregulated in differentiation of human bone marrow-derived mesenchymal stem cells (hMSCs; Liu et al., 2007).

Corin has been studied extensively within the vascular system and is known to regulate blood pressure and sodium homeostasis by activating ANP and brain or B-type natriuretic peptide (BNP; Ichiki, Huntley, & Burnett, 2013; Yan, Wu, Morser, & Wu, 2000). ANP and BNP have previously been shown to modulate angiogenesis and vascular remodelling (Kuhn et al., 2009; Tokudome et al., 2009). In addition, BNP has been linked to regulation of endochondral ossification (Suda et al., 1998) and bone mineral density (Lee et al., 2014). Corin is expressed in developing bone adjacent to the hypertrophic chondrocytes (Yan, Sheng, Seto, Morser, & Wu, 1999), indicating that it may play a role in the regulation of endochondral ossification in developing bone tissue. Moreover, previous studies have reported that serum corin levels are significantly reduced in patients with osteopenia and osteoporosis (Zhou et al., 2013), indicating that corin dysregulation may contribute to certain bone pathologies. However, to date, there has not been an in-depth study to determine corin's role in skeletal biology and osteogenesis.

The goal of this study was to test the hypothesis that corin is a critical regulator of osteogenic differentiation and endochondral ossification via modulation of angiogenic

signalling pathways. To test our hypothesis, we monitored corin expression throughout hASC osteogenic differentiation and knocked down corin expression in hASC to determine its regulatory effect on osteogenic and angiogenic genes. In addition, we used a corin knockout (KO) murine model to evaluate how corin regulates growth plate characteristics in developing long bones, mechanical characteristics of the developing bone, and expression of vascular endothelial growth factor A (VEGF-A) in vivo.

2 | MATERIALS AND METHODS

2.1 | Cell isolation and culture

hASCs were obtained from waste adipose tissue derived from three female donors (ages 25–36) undergoing elective abdominoplasty surgeries (IRB Exemption Protocol #10-0201) at the University of North Carolina hospitals (Chapel Hill, NC). Isolation of hASC was performed as described previously (Bernacki, Wall, & Loboa, 2008; Bodle et al., 2014). Cells were maintained in complete growth medium (CGM, Eagle's minimum essential medium, alpha-modified supplemented with 10% fetal bovine serum, 2 mM L-glutamine, 100 units/ml penicillin, and 100 μg/ml streptomycin), and osteogenic differentiation was induced using osteogenic differentiation medium (ODM, Eagle's minimum essential medium, alpha-modified supplemented with 10% fetal bovine serum, 2 mM L-glutamine, 100 units/ml penicillin and 100 μg/ml streptomycin, 50 μM ascorbic acid, 0.1 μM dexamethasone, and 10 mM β-glycerolphosphate).

2.2 | siRNA knockdown

For knockdown experiments, Stealth RNAi™ siRNA Negative Control Med GC and Corin Stealth RNAi™ siRNA (Thermo Fisher Scientific, Waltham, MA) were used. With the use of an optimized ratio, the following protocol was used to knockdown corin expression: 5 μl of siRNA oligomers, 7.5 μl of Lipofectamine® 2000 (Thermo Fisher Scientific Waltham, MA), and 500 μl OptiMEM (Thermo Fisher Scientific, Waltham, MA) were combined and incubated for 20 min in each well within a six-well plate. hASCs were trypsinized and resuspended at a concentration of 25k/ml in antibiotic free CGM. Of this cell suspension, 2 ml (50k hASC cells) were added to each well. After a 24-hr incubation, the transfection media were replaced with standard CGM or ODM formulations.

2.3 | Osteogenic differentiation evaluation

To evaluate the effect of corin knockdown on hASC, each hASC population was cultured for 14 days in both CGM and ODM, with media changes every 3–4 days. Protein was collected after 14 days of culture in CGM and ODM for quantification. Samples were scraped and suspended in 0.5 ml of Radioimmunoprecipitation assay buffer. Alkaline phosphatase (ALP) activity was quantified with the Alkaline Phosphatase LiquicolorH Test (Stanbio Laboratory, Boerne, TX), using the p-nitrophenylphosphate methodology (Bodle et al., 2013). Protein content was quantified using the bicinchoninic acid absorbance assay (Thermo Fisher Scientific, Waltham, MA), as per manufacturer's protocol.

Gene expression was quantified after 3 days of culture in ODM via quantitative real-time reverse transcription polymerase chain reaction. RNA extraction was carried out using

aTRIzol (Invitrogen, Carlsbad, CA) extraction method using the manufacturer's protocol. RNA concentration and quality were assessed using a NanoDrop spectrophotometer (Thermo Scientific, Wilmington, DE) and reverse transcribed using Marligen's First-strand cDNA Synthesis System (Origene, Rockville, MD). Expression of bone markers osterix (Hs01866874_s1) and runx2 (Hs00231692_m1) and angiogenic marker VEGF-A (Hs00900055_m1) were evaluated usingTaqMan Gene expression assays. All gene expression profiles were normalized to glyceraldehyde-3-phosphate dehydrogenase (Assay HS99999905_M1) in an ABI Prism 7000 system.

2.4 | Histology and growth plate characterization in mice

Wild-type (WT) C57BL/6J mice were purchased from the Jackson Laboratory (Bar Harbor, Maine). Corin KO mice were generated as described previously (Chan et al., 2005) and backcrossed onto the C57BL/6J background. The mice were housed in ventilated cages with a chow diet (Harland Teklad 2918) and freely accessible water at the Cleveland Clinic animal facility with controlled light/dark (12:12 hr) cycles under an approved Institutional Animal Care and Use Committees protocol (#2015-1528). All mouse cages were supplemented with nesting materials and plastic tunnels. Female WT and corin KO mice (10 weeks old) were euthanized by CO_2 inhalation followed by cervical dislocation. Limbs were collected and stored at −80°C for further studies. For histological analysis, tibiae were dissected from corin KO ($n = 8$) and WT ($n = 5$) mice and immediately placed in formalin. After 48 hr, the bones were switched to 70% ethanol and sent to the North Carolina State University College of Veterinary Medicine histology facilities for decalcification, paraffin embedding, sectioning, and haematoxylin and eosin staining. Images of haematoxylin and eosin- stained slides were taken on both a Leica EZD4 histology microscope and a Leica DM5500B microscope using the compatible LAS-AF software (Leica, Wetzlar, Germany). Images were imported to ImageJ Version 10.2, and growth plate thickness was measured at three locations from each specimen as technical triplicates before statistics were performed.

2.5 | Immunohistochemistry

Additional paraffin-embedded slides were used for immunohistochemistry ($n = 3$ WT, $n = 3$ corin KO). The protocol used was adapted from previously described methods (Puetzer, Brown, Ballyns, & Bonassar, 2013) In brief, slides were deparaffinized and washed for 20 min in 10 mM citrate antigen retrieval buffer heated to 90°C. The slides were then washed for 10 min in 1× Tris–buffer saline/0.5% Tween 20 solution, 30 min in a solution of 37 units/ml hyaluronidase, and 30 min in a 3% hydrogen peroxide solution, and the slides were blocked with a normal goat serum solution for 1 hr. Samples were incubated at room temperature for 2 hr in a 1:200 dilution primary antibody solution (rabbit polyclonal anti-VEGF-A, Abcam, Cambridge, United Kingdom). The samples were washed with phosphate-buffered saline (PBS) and incubated in secondary solution for 1 hr (goat antirabbit IgG H&L HRP polymer, Abcam). The slides were stained with a DAB Substrate Kit (Abcam) for 10 min and imaged with a Leica DM5500B microscope (Leica, Wetzlar, Germany).

2.6 | Mechanical testing

Three-point-bending tests were carried out as described previously (Jepsen, Silva, Vashishth, Guo, & van der Meulen, 2015; Turner & Burr, 1993). Briefly, femurs were dissected from corin KO ($n = 8$) and WT ($n = 5$) mice. Lengths and diameters at the centres of each femur were recorded. Femurs were wrapped in PBS-soaked paper towels and frozen at $-25°C$ until testing. To thaw bones for testing, femurs were placed in room-temperature PBS. All testing was carried out on a Bose EnduraTEC ELF3220 (EnduraTEC Systems Corp., Minnetonka, MN) equipped with a 50-lb load cell (Model 31/1430-05, Sensotec, Columbus, OH). The test fixture was set with 6-mm spacing between the two end supports. The femurs were place into the loading fixture with the anterior face upwards and loaded from the top in an anterior to posterior direction. A 0.05-N preload was placed on the femurs before the test began. Once set up, the specimens were loaded at a rate of 0.05 mm/s. Specimens were kept moistened throughout the testing duration. Force and displacement measurements were recorded and exported to MS Excel for analysis. Stiffness was determined by fitting a trend line to the initial linear region of the load–displacement curve. Maximum load was determined as the greatest load force recorded in a data set prior to specimen failure. Yield point was defined as the point where the data set intersected with the stiffness line multiplied by 0.9. Yield point deflection was the difference between the defection at failure and the deflection at yield. The work to fracture was calculated by integrating the data to find the total area under the load displacement curve.

2.7 | Statistical analyses

Paired Student t tests were used to compare corin knockdown versus control knockdown and corin KO versus WT data. Corin time course data were analysed using one-way analysis of variance with Tukey post hoc analyses. Data were log transformed before running analyses. A level of $p < 0.05$ was considered significant. Significance is denoted throughout this study as $*p < 0.05$ and $**p < 0.01$. All data are presented as average with error bars representing standard error of the mean.

3 | RESULTS

3.1 | Corin expression is increased during osteogenic differentiation of hASC

Corin expression was highly upregulated throughout osteogenic differentiation of hASC in all three donors (Figure 1a–c). Comparison of CGM and ODM corin expression levels showed significantly higher expression in ODM at all time points ($p < 0.05$). Donor-to-donor variability was observed within the corin expression profiles of each donor. Donor 1 expression peaked at Day 7, donor 2 expression peaked at Day 10, and donor 3 expression peaked at Days 10 and 14.

3.2 | Corin knockdown modulated characteristics osteogenic differentiation in hASC

When the knockdown was evaluated via polymerase chain reaction 72 hr after transfection, approximately 60% knockdown efficiency was observed ($p < 0.01$; Figure 1d). Total protein content assessed at Day 14 was significantly decreased in both CGM and ODM of all three donors. Protein content was normalized to CGM control knockdown levels for each line.

When corin was knocked down, there was a significant decrease in protein content from hASC cultured in both CGM and ODM (Figure 1e). Endogenous ALP activity per microgram protein content was calculated and normalized to control knockdown levels for each donor line. ALP activity was significantly decreased with corin knockdown ($p < 0.05$; Figure 1f). Corin knockdown during hASC osteogenic differentiation did not alter expression patterns of bone markers osterix (Figure 1g) or runx2 (Figure 1h). However, corin knockdown significantly increased VEGF-A mRNA expression during osteogenic differentiation of hASC in all three donors (Figure 1i).

3.3 | Corin KO altered endochondral ossification patterns in vivo

Endochondral ossification was altered within corin KO bones. Growth plate thickness was much greater in WT than corin KO tibiae (Figure 2a,b). The trabeculae and bone marrow patterning was altered with a reduction in the primary spongiosa of the KO tibia. When the growth plate thicknesses were quantified, the reduction in growth plate thickness was statistically significant ($p < 0.01$; Figure 2c). The hypertrophic chondrocyte regions observed in the WT growth plates were severely reduced in corin KO tibiae (Figure 2d,e).

3.4 | Corin KO altered functional characteristics of bone in vivo

Femur length was increased from 14.0 to 15.7 mm in corin KO femurs relative to WT ($p < 0.01$; Figure 3a), but femur diameter was not altered (Figure 3b). Load–displacement curves from WT and corin KO three-point-bending tests show altered mechanics in corin KO femurs (Figure 3c). When quantified, there was a statistically significant increase in maximum load from 11.1 to 17.4 N in the corin KO femurs ($p < 0.01$; Figure 3d). In addition, stiffness was increased from 65.3 to 121 N/mm in corin KO femurs ($p < 0.01$; Figure 3e). Postyield deflection was significantly decreased from 1.2 to 0.6 mm in corin KO femurs relative to WT ($p < 0.01$; Figure 3f). However, work to fracture was similar between both groups (Figure 3g).

3.5 | Corin KO altered VEGF-A expression in vivo

In order to determine if corin regulates VEGF-A expression patterns in vivo, immunohistochemistry was used to visualize VEGF-A localization. We found that VEGF-A expression was altered in corin KO tibiae (Figure 4). In comparison with WT tibiae, corin KO tibiae exhibited increased VEGF-A expression adjacent to the growth plate. However, the tibial shaft of WT mice had greater VEGF-A expression than had that of corin KO mice. No VEGF-A expression was observed in the distal end of the tibia in corin KO mice, but VEGF-A staining was clearly observed in the distal end of the tibia in WT mice.

4 | DISCUSSION

The objective of this study was to determine if corin regulates bone development and to determine the mechanism(s) through which corin may act. We found that corin is highly upregulated during osteogenic differentiation with a greater than 200-fold increase in corin expression in hASC of all donors assessed. Corin siRNA knockdown elevated VEGF-A expression during osteogenic differentiation in vitro. When corin was knocked out in a murine model, we saw developmental changes to the bone structure at both the tissue and

cellular levels. Further, the width of the growth plate was significantly reduced in corin KO mice, and the hypertrophic zone was nearly absent. Femur stiffness and maximum load were increased in corin KO mice, but postyield deflection was significantly reduced, suggesting that corin KO femurs are more brittle than WT femurs. In addition, corin KO mice expressed more VEGF-A at the growth plate but decreased VEGF-A expression throughout the length of the tibial shaft and distal femoral head relative to WT controls. Overall, this suggests that corin regulates bone development via modulation of VEGF-A expression.

To our knowledge, this is the first study to show that corin regulates skeletal development. Previously, there has been conflicting evidence on whether corin is expressed in skeletal tissue (Hooper, Scarman, Clarke, Normyle, & Antalis, 2000; Yan et al., 1999). Corin mRNA expression was observed via in situ hybridization in developing mouse bone. Specifically, corin was expressed in the region adjacent to hypertrophic chondrocytes and in perichondrocytes (Yan et al., 1999). However, corin was not detected via immunohistological analyses in human skeletal tissue (Hooper et al., 2000). This could potentially be because corin is only expressed during skeletal development, supported by our finding that corin expression was absent during hASC culture in CGM. We previously reported an increase in corin expression during osteogenic differentiation of hASC (Charoenpanich et al., 2011). In addition, it was recently reported that corin modulates chondrogenic differentiation in hMSCs (Zhou, Zhu, Liu, Wu, & Dong, 2017). In this study, we verified that corin was highly expressed throughout osteogenic differentiation in three separate hASC cell populations. We have also previously reported that hASCs differentiate at different rates (Nordberg et al., 2017). In this study, we observed different corin expression profiles amongst the three donors, likely due to temporal variability in the onset of osteogenic differentiation between the donors' hASCs. In addition, we report that corin knockdown reduces endogenous ALP activity, a marker for osteogenic differentiation, suggesting that corin is actively involved in the process of osteogenesis and is not merely passively upregulated.

Corin KO mice have been reported to develop normally and are fertile (Chan et al., 2005). However, corin KO mice have a slightly elevated body mass and a propensity develop hypertension (Chan et al., 2005; Wang et al., 2012; Wang et al., 2012). In addition, pregnant corin KO mice develop characteristics of pre-eclampsia (Cui et al., 2012). In this study, altered bone properties are observed within corin KO mice. Here, we show that corin KO reduced the width of the hypertrophic zone, but femur length was slightly increased. This suggests that the rate of endochondral ossification progression was not hindered by the loss of corin. Rather, our data suggest that endochondral ossification is held in check by corin, and the loss of corin yields unregulated bone growth. Three-point-bending tests were used to evaluate mechanical properties of the corin KO femurs. An increase in stiffness and maximum load to failure were observed in corin KO femurs. This suggests that cortical properties of corin KO femurs are altered relative to WT controls. However, corin KO reduced postyield deflection, indicating that corin KO femurs are more brittle than WT femurs. Although at this point purely speculative, the altered mechanical properties of corin KO long bones could be caused by the dysregulation of collagen expression in corin KO bones. Mechanical properties of bone are derived from both hydroxyapatite, to provide compressive strength, and collagen fibres, to provide tensile strength and prevent brittle

fracture (Fung, 1993). Mice that only express the VEGF120 isoform of VEGF-A have been documented to have abnormal collagen expression and vascularization patterns in developing long bones (Zelzer et al., 2002). VEGF-A dysregulation in the current study may have altered the collagen composition of the bones yielding KO long bones that were more brittle than the WT controls. Taken together, the results of this study demonstrate that corin appears to be critical for normal bone formation.

Although corin has not been previously implicated in the regulation of endochondral ossification, natriuretic peptides have been suggested to play a role in skeletal biology and endochondral ossification (Chusho et al., 2001; Komatsu et al., 2002; Lee et al., 2014; Pejchalova, Krejci, & Wilcox, 2007; Suda et al., 1998; Teixeira, Agoston, & Beier, 2008). Within cardiac research, corin has been shown to cleave the precursors pro-ANP and pro-BNP into active ANP and BNP, respectively (Ichiki et al., 2013; Semenov et al., 2010; Yan et al., 2000, Zhou & Wu, 2014). It has been shown that BNP regulates endochondral ossification and BNP overexpression can lead to skeletal overgrowth (Suda et al., 1998). It has also been reported that BNP transgenic mice exhibit increased hypertrophic zone width (Chusho et al., 2000). Skeletal abnormalities were not reported in BNP KO mice (Tamura et al., 2000), although hypertrophic widths were not compared with those of WT mice. In addition, N-terminal pro-BNP serum levels have been shown to be negatively correlated with lumbar bone mineral density (Lee et al., 2014). C-type natriuretic peptide (CNP), also critical to regulation of bone development, has been shown to regulate endochondral ossification (Komatsu et al., 2002). Mice deficient in CNP demonstrated a narrowing of the growth plate and a reduced hypertrophic zone during long bone development (Chusho et al., 2001; Komatsu et al., 2002), similar to the corin KO phenotype described in the present study. A major difference between mice deficient in CNP and corin is that CNP KO mice exhibit dwarfism (Chusho et al., 2001) whereas corin KO mice have slightly elongated femurs. Although CNP is a mediator of endochondral ossification, to date, there has been no evidence that corin processes pro‐ CNP to active CNP (Zhou & Wu, 2014). Rather, furin is considered the major pro‐CNP processor (Wu, Wu, Pan, Morser, & Wu, 2003). However, our previous microarray study did not detect an increase in furin expression during osteogenic differentiation (Charoenpanich et al., 2011; Charoenpanich et al., 2014). Although it is likely that corin interacts with BNP and/or CNP within long bone development, the precise mechanism of action remains to be determined.

Due to corin's role in vascular biology and the role that natriuretic peptides have been suggested to play in endochondral ossification, we investigated whether corin modulates the expression of a major regulator of angiogenesis, VEGF-A. We knocked down corin expression via siRNA to determine if expression patterns of bone markers osterix or runx2 were altered. No significant change was observed in runx2 expression in the hASC of any donor. Only one donor showed a significant change in osterix expression. These data are consistent with those of previous research that found no difference in bone markers when corin was silenced in hMSCs (Zhou et al., 2017). However, VEGF-A expression was significantly upregulated when corin expression was knocked down in all hASC populations. This suggests that corin is involved in the regulation of angiogenic signalling pathways during osteogenic differentiation rather than traditional bone markers. In vivo, an increase in VEGF-A protein expression was observed in corin KO mice adjacent to the hypertrophic

zone. Corin mRNA has previously been detected via in situ hybridization in the region adjacent to the hypertrophic zone in developing mice (Yan et al., 1999). Taken together, this would suggest that corin modulates local VEGF- A expression. The observed increase in VEGF-A expression near the growth plate in corin KO mice could explain the reduced width of the hypertrophic zone by promoting premature angiogenesis and ossification of the terminal hypertrophic chondrocytes.

VEGF-A is important for the initiation of blood vessel formation within the hypertrophic zone (Yang et al., 2012; Zelzer et al., 2004). VEGF-A conditional KO mice have been previously shown to have wider hypertrophic zones because lack of VEGF-A delays the removal of hypertrophic chondrocytes from the hypertrophic zone (Zelzer et al., 2004). Although VEGF-A expression was elevated at the growth plate, throughout the tibial shaft and proximal tibial head, VEGF-A expression was markedly reduced in corin KO mice. As normal vascular function within bone is imperative for successful fracture healing (Bahney, Hu, Miclau, & Marcucio, 2015), this dysregulation of VEGF- A expression may prevent proper bone healing in corin-deficient mice. Interestingly, deregulation of VEGF-A is a hallmark of pre-eclampsia (Tsatsaris et al., 2003), a pathology that has also been tied to the corin-ANP pathway. Specifically, the corin-ANP pathway has been shown to regulate trophoblast invasion and uterine spiral artery remodelling, and dysregulation in this pathway contributes to pre-eclampsia (Cui et al., 2012). Whether or not corin contributes to VEGF-A dysregulation in pre-eclampsia has yet to be determined. Although the current study suggests that Corin is a key regulator of endochondral ossification via regulation of VEGF-A expression, the exact mechanism of this interaction has yet to be fully elucidated. Future work should investigate how corin KO affects markers of hypertrophy and osteogenesis in vivo.

In conclusion, our data suggest that absence of corin leads to premature angiogenesis and ossification of the terminal hypertrophic chondrocytes. This dysregulation causes skeletal overgrowth, abnormal bone patterning, altered bone mechanical properties, and dysregulated VEGF-A expression. To our knowledge, this is the first study to find that corin appears to be a key regulator of bone development by modulating VEGF-A expression. Although more research is needed to fully elucidate this mechanism, our findings have several potential scientific implications and potential therapeutic applications such as targeting corin to prevent ossification of cartilage in osteoarthritis or using corin expression to control angiogenesis in tissue engineered bone constructs.

ACKNOWLEDGEMENTS

REFERENCES

Bahney CS, Hu DP, Miclau T 3rd, & Marcucio RS (2015). The multifaceted role of the vasculature in endochondral fracture repair. Front Endocrinol (Lausanne), 6, 4 10.3389/fendo.2015.00004 [PubMed: 25699016]

Bernacki SH, Wall ME, & Loboa EG (2008). Isolation of human mesenchymal stem cells from bone and adipose tissue. Methods in Cell Biology, 86, 257–278. 10.1016/S0091-679X(08)00011-3 [PubMed: 18442651]

Bodle JC, Rubenstein CD, Phillips ME, Bernacki SH, Qi J, Banes AJ, & Loboa EG (2013). Primary cilia: The chemical antenna regulating human adipose-derived stem cell osteogenesis. PLoS One, 8, e62554 10.1371/journal.pone.0062554 [PubMed: 23690943]

Bodle JC, Teeter SD, Hluck BH, Hardin JW, Bernacki SH, & Loboa EG (2014). Age-related effects on the potency of human adipose-derived stem cells: Creation and evaluation of superlots and implications for musculoskeletal tissue engineering applications. Tissue Engineering. Part C, Methods, 20, 972–983. 10.1089/ten.tec.2013.0683 [PubMed: 24628423]

Chan JC, Knudson O, Wu F, Morser J, Dole WP, & Wu Q (2005). Hypertension in mice lacking the proatrial natriuretic peptide convertase corin. Proceedings of the National Academy of Sciences of the United States of America, 102, 785–790. 10.1073/pnas.0407234102 [PubMed: 15637153]

Charoenpanich A, Wall ME, Tucker CJ, Andrews DM, Lalush DS, Dirschl DR, & Loboa EG (2014). Cyclic tensile strain enhances osteogenesis and angiogenesis in mesenchymal stem cells from osteoporotic donors. Tissue Engineering. Part A, 20, 67–78. 10.1089/ten.tea.2013.0006 [PubMed: 23927731]

Charoenpanich A, Wall ME, Tucker CJ, Andrews DM, Lalush DS, & Loboa EG (2011). Microarray analysis of human adipose-derived stem cells in three-dimensional collagen culture: osteogenesis inhibits bone morphogenic protein and Wnt signaling pathways, and cyclic tensile strain causes upregulation of proinflammatory cytokine regulators and angiogenic factors. Tissue Engineering. Part A, 17, 2615–2627. 10.1089/ten.tea.2011.0107 [PubMed: 21767168]

Chusho H, Ogawa Y, Tamura N, Suda M, Yasoda A, Miyazawa T, … Nakao K (2000). Genetic models reveal that brain natriuretic peptide can signal through different tissue-specific receptor-mediated pathways. Endocrinology, 141, 3807–3813. 10.1210/endo.141.10.7692 [PubMed: 11014237]

Chusho H, Tamura N, Ogawa Y, Yasoda A, Suda M, Miyazawa T, … Nakao K (2001). Dwarfism and early death in mice lacking C-type natriuretic peptide. Proceedings of the National Academy of Sciences of the United States of America, 98, 4016–4021. 10.1073/pnas.071389098 [PubMed: 11259675]

Cui Y, Wang W, Dong N, Lou J, Srinivasan DK, Cheng W, … Wu Q (2012). Role of corin in trophoblast invasion and uterine spiral artery remodelling in pregnancy. Nature, 484, 246–250. 10.1038/nature10897 [PubMed: 22437503]

Fung YC (1993). In Yuan-Cheng Y (Ed.), Biomechanics: Mechanical properties of living tissue (pp. 500–536). Springer-Verlag 10.1007/978-1-4757-2257-4_12

Gimble JM, Katz AJ, & Bunnell BA (2007). Adipose-derived stem cells for regenerative medicine. Circulation Research, 100, 1249–1260. 10.1161/01.RES.0000265074.83288.09 [PubMed: 17495232]

Gomillion CT, & Burg KJ (2006). Stem cells and adipose tissue engineering. Biomaterials, 27, 6052–6063. 10.1016/j.biomaterials.2006.07.033 [PubMed: 16973213]

Hooper JD, Scarman AL, Clarke BE, Normyle JF, & Antalis TM (2000). Localization of the mosaic transmembrane serine protease corin to heart myocytes. European Journal of Biochemistry, 267, 6931–6937. 10.1046/j.1432-1033.2000.01806.x [PubMed: 11082206]

Ichiki T, Huntley BK, & Burnett JC Jr. (2013). BNP molecular forms and processing by the cardiac serine protease corin. Advances in Clinical Chemistry, 61, 1–31. 10.1016/B978-0-12-407680-8.00001-4 [PubMed: 24015598]

Jepsen KJ, Silva MJ, Vashishth D, Guo XE, & van der Meulen MC (2015). Establishing biomechanical mechanisms in mouse models: Practical guidelines for systematically evaluating phenotypic

changes in the diaphyses of long bones. Journal of Bone and Mineral Research, 30, 951–966. 10.1002/jbmr.2539 [PubMed: 25917136]

Komatsu Y, Chusho H, Tamura N, Yasoda A, Miyazawa T, Suda M, … Nakao K (2002). Significance of C-type natriuretic peptide (CNP) in endochondral ossification: analysis of CNP knockout mice. Journal of Bone and Mineral Metabolism, 20, 331–336. 10.1007/s007740200048 [PubMed: 12434160]

Kuhn M, Volker K, Schwarz K, Carbajo-Lozoya J, Flogel U, Jacoby C, … Baba HA (2009). The natriuretic peptide/guanylyl cyclase—A system functions as a stress-responsive regulator of angiogenesis in mice. The Journal of Clinical Investigation, 119, 2019–2030. 10.1172/JCI37430 [PubMed: 19487812]

Lee MC, Lee CJ, Shih MH, Ho GJ, Chen YC, & Hsu BG (2014). N-terminal pro-B-type natriuretic peptide is inversely related to bone mineral density in renal transplant recipients. Transplantation Proceedings, 46, 3443–3447. 10.1016/j.transproceed.2014.06.077 [PubMed: 25498069]

Lee RH, Kim B, Choi I, Kim H, Choi HS, Suh K, … Jung JS (2004). Characterization and expression analysis of mesenchymal stem cells from human bone marrow and adipose tissue. Cellular Physiology and Biochemistry, 14, 311–324. 10.1159/000080341 [PubMed: 15319535]

Liu TM, Martina M, Hutmacher DW, Hui JH, Lee EH, & Lim B (2007). Identification of common pathways mediating differentiation of bone marrow-and adipose tissue-derived human mesenchymal stem cells into three mesenchymal lineages. Stem Cells, 25, 750–760. 10.1634/stemcells.2006-0394 [PubMed: 17095706]

Mackie EJ, Ahmed YA, Tatarczuch L, Chen KS, & Mirams M (2008). Endochondral ossification: How cartilage is converted into bone in the developing skeleton. The International Journal of Biochemistry & Cell Biology, 40, 46–62. 10.1016/j.biocel.2007.06.009

Mizuno H (2009). Adipose-derived stem cells for tissue repair and regeneration: Ten years of research and a literature review. Journal of Nippon Medical School, 76, 56–66. 10.1272/jnms.76.56 [PubMed: 19443990]

Nordberg RC, & Loboa EG (2015). Our fat future: Translating adipose stem cell therapy. Stem Cells Translational Medicine, 4, 974–979. 10.5966/sctm.2015-0071 [PubMed: 26185256]

Nordberg RC, Zhang J, Griffith EH, Frank MW, Starly B, & Loboa EG (2017). Electrical cell-substrate impedance spectroscopy can monitor age-grouped human adipose stem cell variability during osteogenic differentiation. Stem Cells Translational Medicine, 6, 502–511. 10.5966/sctm.2015-0404 [PubMed: 28191763]

Pejchalova K, Krejci P, & Wilcox WR (2007). C-natriuretic peptide: An important regulator of cartilage. Molecular Genetics and Metabolism, 92, 210–215. 10.1016/j.ymgme.2007.06.014 [PubMed: 17681481]

Puetzer JL, Brown BN, Ballyns JJ, & Bonassar LJ (2013). The effect of IGF-I on anatomically shaped tissue-engineered menisci. Tissue Engineering. Part A, 19, 1443–1450. 10.1089/ten.tea.2012.0645 [PubMed: 23360441]

Schaffler A, & Buchler C (2007). Concise review: adipose tissue-derived stromal cells—Basic and clinical implications for novel cell-based therapies. Stem Cells, 25, 818–827. 10.1634/stemcells.2006-0589 [PubMed: 17420225]

Semenov AG, Tamm NN, Seferian KR, Postnikov AB, Karpova NS, Serebryanaya DV, … Katrukha AG (2010). Processing of pro-B-type natriuretic peptide: Furin and corin as candidate convertases. Clinical Chemistry, 56, 1166–1176. 10.1373/clinchem.2010.143883 [PubMed: 20489134]

Suda M, Ogawa Y, Tanaka K, Tamura N, Yasoda A, Takigawa T, … Nakao K (1998). Skeletal overgrowth in transgenic mice that overexpress brain natriuretic peptide. Proceedings of the National Academy of Sciences of the United States of America, 95, 2337–2342. 10.1073/pnas.95.5.2337 [PubMed: 9482886]

Tamura N, Ogawa Y, Chusho H, Nakamura K, Nakao K, Suda M, … Katsuki M (2000). Cardiac fibrosis in mice lacking brain natriuretic peptide. Proceedings of the National Academy of Sciences of the United States of America, 97, 4239–4244. 10.1073/pnas.070371497 [PubMed: 10737768]

Teixeira CC, Agoston H, & Beier F (2008). Nitric oxide, C-type natriuretic peptide and cGMP as regulators of endochondral ossification. Developmental Biology, 319, 171–178. 10.1016/j.ydbio. 2008.04.031 [PubMed: 18514181]

Tokudome T, Kishimoto I, Yamahara K, Osaki T, Minamino N, Horio T, … Kangawa K (2009). Impaired recovery of blood flow after hind-limb ischemia in mice lacking guanylyl cyclase-A, a receptor for atrial and brain natriuretic peptides. Arteriosclerosis, Thrombosis, and Vascular Biology, 29, 1516–1521. 10.1161/ATVBAHA.109.187526

Tsatsaris V, Goffin F, Munaut C, Brichant JF, Pignon MR, Noel A, … Foidart JM (2003). Overexpression of the soluble vascular endothelial growth factor receptor in preeclamptic patients: Pathophysiological consequences. The Journal of Clinical Endocrinology and Metabolism, 88, 5555–5563. 10.1210/jc.2003-030528 [PubMed: 14602804]

Turner CH, & Burr DB (1993). Basic biomechanical measurements of bone: A tutorial. Bone, 14, 595–608. 10.1016/8756-3282(93)90081-K [PubMed: 8274302]

Wang W, Cui Y, Shen J, Jiang J, Chen S, Peng J, & Wu Q (2012). Salt-sensitive hypertension and cardiac hypertrophy in transgenic mice expressing a corin variant identified in blacks. Hypertension, 60, 1352–1358. 10.1161/HYPERTENSIONAHA.112.201244 [PubMed: 22987923]

Wang W, Shen J, Cui Y, Jiang J, Chen S, Peng J, & Wu Q (2012). Impaired sodium excretion and salt-sensitive hypertension in corin-deficient mice. Kidney International, 82, 26–33. 10.1038/ki. 2012.41 [PubMed: 22418978]

Wu C, Wu F, Pan J, Morser J, & Wu Q (2003). Furin-mediated processing of Pro-C-type natriuretic peptide. The Journal of Biological Chemistry, 278, 25847–25852. 10.1074/jbc.M301223200 [PubMed: 12736257]

Yan W, Sheng N, Seto M, Morser J, & Wu Q (1999). Corin, a mosaic transmembrane serine protease encoded by a novel cDNA from human heart. The Journal of Biological Chemistry, 274, 14926–14935. 10.1074/jbc.274.21.14926 [PubMed: 10329693]

Yan W, Wu F, Morser J, & Wu Q (2000). Corin, a transmembrane cardiac serine protease, acts as a pro-atrial natriuretic peptide-converting enzyme. Proceedings of the National Academy of Sciences of the United States of America, 97, 8525–8529. 10.1073/pnas.150149097 [PubMed: 10880574]

Yang YQ, Tan YY, Wong R, Wenden A, Zhang LK, & Rabie AB (2012). The role of vascular endothelial growth factor in ossification. International Journal of Oral Science, 4, 64–68. 10.1038/ijos.2012.33 [PubMed: 22722639]

Zelzer E, Mamluk R, Ferrara N, Johnson RS, Schipani E, & Olsen BR (2004). VEGFA is necessary for chondrocyte survival during bone development. Development, 131, 2161–2171. 10.1242/dev. 01053 [PubMed: 15073147]

Zelzer E, McLean W, Ng YS, Fukai N, Reginato AM, Lovejoy S, … Olsen BR (2002). Skeletal defects in VEGF(120/120) mice reveal multiple roles for VEGF in skeletogenesis. Development, 129, 1893–1904. [PubMed: 11934855]

Zhou H, Liu W, Zhu J, Liu M, Fang C, Wu Q, & Dong N (2013). Reduced serum corin levels in patients with osteoporosis. Clinica Chimica Acta, 426, 152–156. 10.1016/j.cca.2013.09.007

Zhou H, Zhu J, Liu M, Wu Q, & Dong N (2017). Role of the protease corin in chondrogenic differentiation of human bone marrow-derived mesenchymal stem cells. Journal of Tissue Engineering and Regenerative Medicine. 10.1002/term.2514

Zhou Y, & Wu Q (2014). Corin in natriuretic peptide processing and hypertension. Current Hypertension Reports, 16(415). 013–0415-7. 10.1007/s11906-013-0415-7
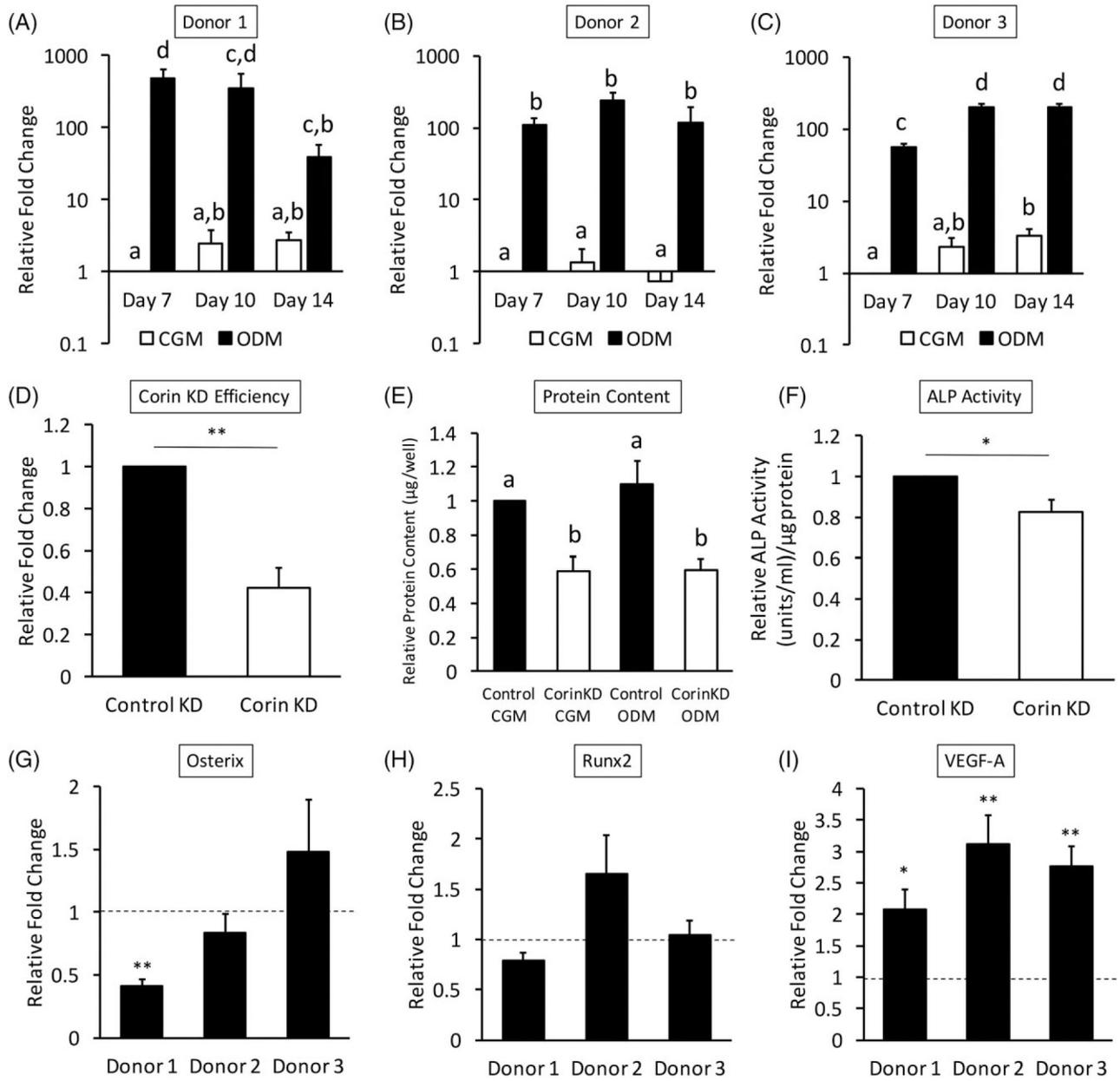
FIGURE 1.

Corin mRNA expression was highly upregulated throughout culture in osteogenic differentiation medium (ODM) in all three donors (a–c; different uppercase letters indicate that data are significantly different, $p < 0.05$). All data was normalized to Day 7 culture of hASC in complete growth medium (CGM), and statistics were run on log-transformed data with a significance level set to $p < 0.05$. Different uppercase letters indicate statistical difference. (d) Corin knockdown efficiency was evaluated 72 hr after transfection (**$p < 0.01$). (e) Corin knockdown decreased total protein levels of hASC cultured in CGM and ODM after 14 days. Data are normalized to CGM control protein levels for each donor line and expressed as a per cent of the control levels. A significance level was set to $p < 0.05$, and different uppercase letters indicate statistical difference. Corin knockdown gene expression

was evaluated after 3 days of hASC culture in osteogenic differentiation medium (ODM).(f) Endogenous alkaline phosphatase (ALP) activity in active units per microgram protein content was significantly decreased when corin was knocked down. Data were normalized to control knockdown levels for each donor line (*$p < 0.05$). Osteogenic markers (g) osterix and (h) runx2 did not show a clear trend when corin was knocked down. (i) Vascular endothelial growth factor A (VEGF-A) expression significantly increased with corin knockdown in all three donors. Data were normalized to control knockdown expression levels (dashed line). Statistics compare corin knockdown versus control knockdown (*$p < 0.05$, **$p < 0.01$)
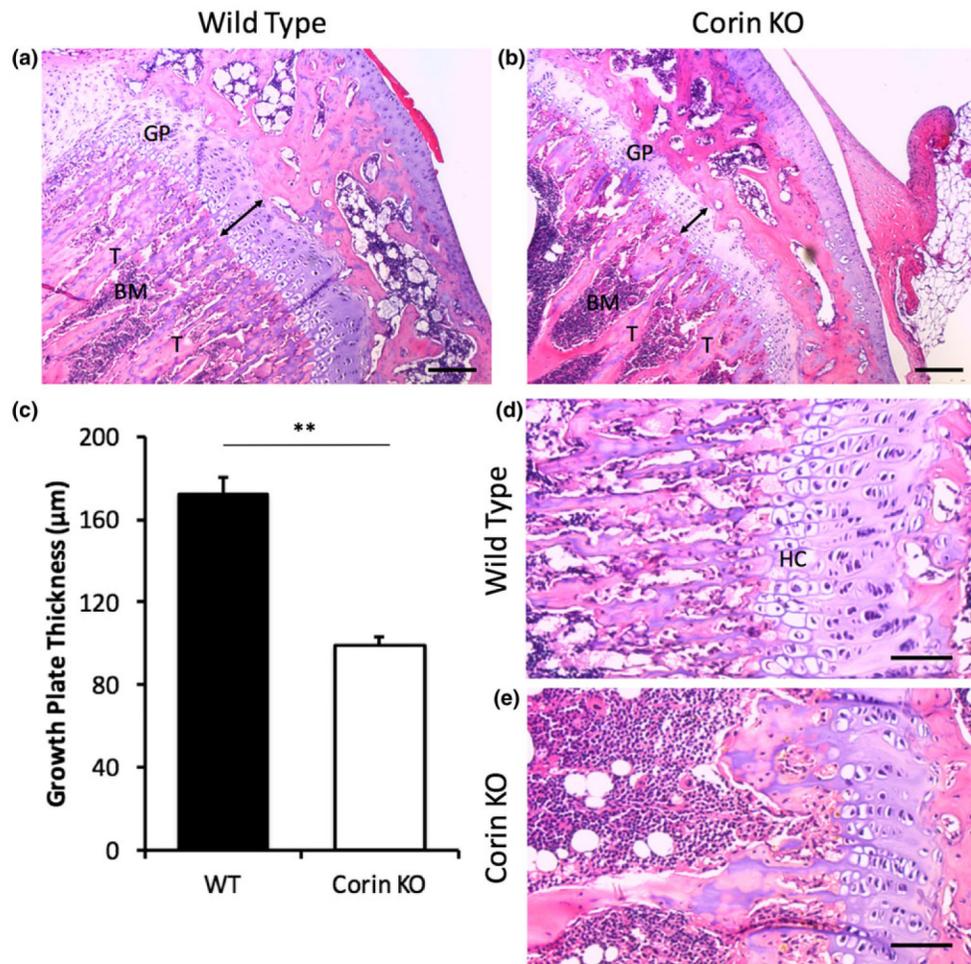
FIGURE 2.

Endochondral ossification was altered within corin knockout (KO) bones. Growth plate thickness was much greater in wild-type (WT; $n = 5$; a) than corin KO ($n = 8$; b) tibiae (scale bars = 150 μm). (c) When quantified, this trend was statistically significant (** $p < 0.01$). The hypertrophic chondrocyte regions observed in the WT growth plates (d) were significantly reduced in corin KO tibiae (e; scale bars = 75 μm). Figure abbreviations: GP = growth plate, BM = bone marrow, T = trabeculae, HC = hypertrophic chondrocytes
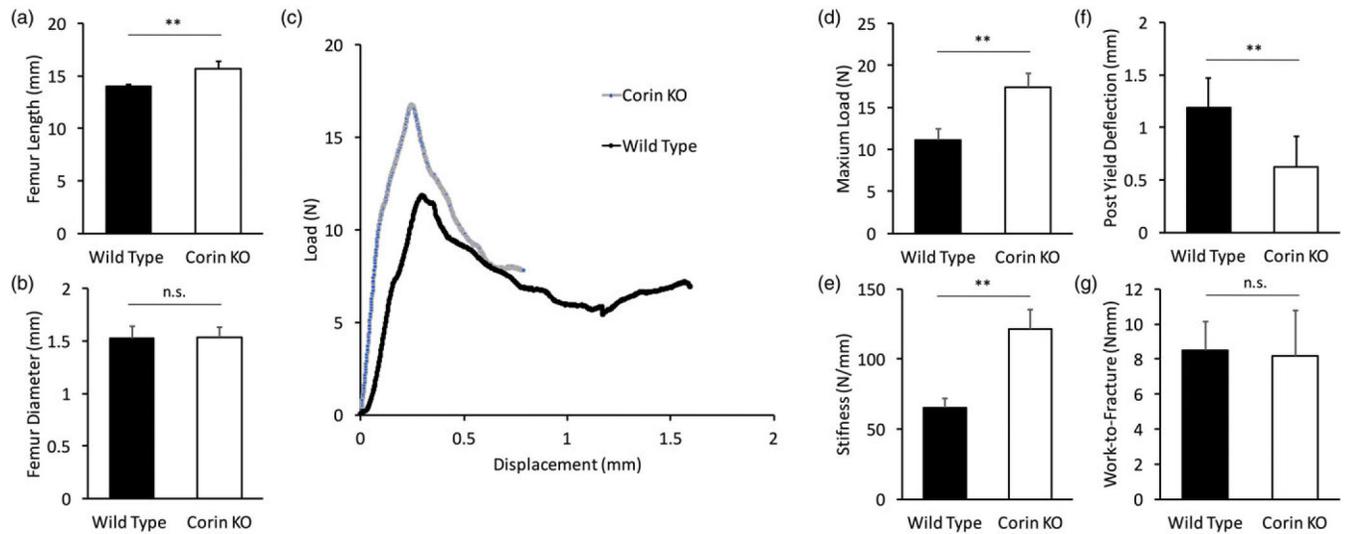
FIGURE 3.

Mechanical properties were altered in corin knockout (KO) femurs. (a) Femurs in corin KO mice were longer than those of wild-type mice, but (b) femur diameter was not affected. (c) Representative data sets of three-point-bending tests from both corin KO and wild-type mice show that corin KO femurs were stiffer and more brittle than were wild-type femurs. When quantified, corin KO femurs exhibited significantly greater (d) maximum loads and (e) stiffnesses relative to wild-type femurs. (f) Postyield deflection was significantly decreased in corin KO femurs, but (g) work to fracture was similar between both groups. (**$p < 0.01$, n.s. = not significant)
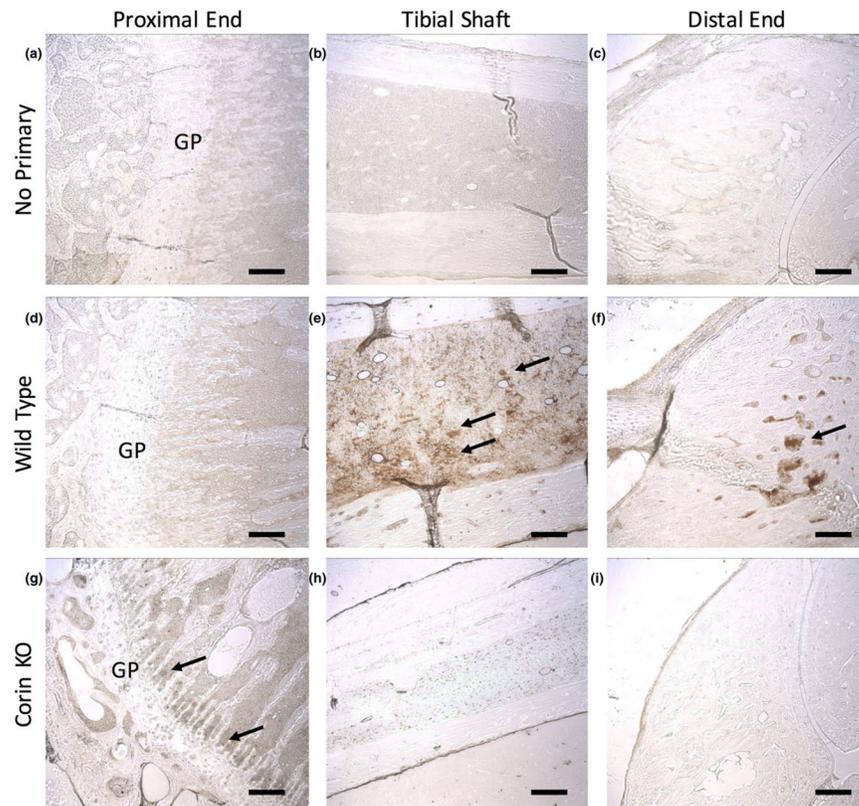
FIGURE 4.

Vascular endothelial growth factor A (VEGF-A) expression was altered in corin knockout (KO) tibiae. (a–c) No background secondary staining was observed in sections stained without the primary antibody. In comparison with (d) wild-type tibiae, (g) corin KO tibiae exhibited increased VEGF-A expression (arrows, brown colour) adjacent to the growth plate. However, (e) the tibial shafts of wild-type mice had greater VEGF-A expression than (h) had those of corin KO mice. (i) No VEGF-A expression was observed in the distal end of the tibia in corin KO mice, but (f) VEGF-A staining was clearly observed in the distal end of the tibia in wild-type mice. Figure abbreviation: GP = growth plate. All scale bars = 150 µm